HUMAN GENE THERAPY 10:591–602 (March 1, 1999)
Mary Ann Liebert, Inc.

Two Independent Molecular Pathways for Recombinant Adeno-Associated Virus Genome Conversion Occur after UV-C and E4orf6 Augmentation of Transduction

SALIH SANLIOGLU, DONGSHENG DUAN, and JOHN F. ENGELHARDT

ABSTRACT

Numerous environmental influences have been demonstrated to enhance recombinant adeno-associated virus (rAAV) transduction. Such findings are the foundation of developing new and innovative strategies to improve the efficiency of rAAV as a gene therapy vector. Several of these environmental factors included genotoxic stresses such as UV and γ irradiation as well as certain adenoviral gene products such as E4orf6. The mechanisms by which these environmental stimuli increase rAAV transduction are only partially understood but have been suggested to involve both endocytosis and uptake of virus to the nucleus, as well as conversion of single-stranded DNA viral genomes to double-stranded expressible forms. Two molecular intermediates of rAAV genomes, which have been demonstrated to correlate with transgene expression and/or the persistence of rAAV, include both replication form (Rf) monomers and dimers as well as circular intermediates. In the present study, we demonstrate that augmentation of rAAV transduction by UV irradiation and the adenoviral protein E4orf6 correlates with distinct increases in either circular or replication form intermediates, respectively. UV irradiation of primary fibroblasts at 15 J/m^2 resulted in a 15-fold induction of head-to-tail circular intermediates, with minimal induction of replication form rAAV genomes. In contrast, E4orf6-augmented rAAV transduction was correlated with the formation of replication form intermediates, with no alteration in the abundance of circular intermediates. These findings demonstrate that rAAV transduction can occur through two independent molecular pathways that convert single-stranded AAV genomes to expressible forms of DNA.

OVERVIEW SUMMARY

Adenovirus E4orf6 gene expression has been demonstrated to enhance rAAV transduction, leading to augmentation of replication form intermediates. Similarly, DNA-damaging agents such as ionizing radiation, hydroxyurea, and UV have also been shown to increase gene expression following rAAV infection. Central to the development of rAAV as a gene therapy vector is a better understanding of these mechanisms that can augment rAAV transduction and application of this knowledge in more effective strategies for *in vivo* gene transfer. In the present article, we describe two types of environmental stimuli that augment rAAV transduction through distinct molecular pathways. Specifically, UV-C irradiation produced substantial augmentation of rAAV circular form genomes, with little enhancement of replicative form genomes. In contrast, replication-defective adenovirus expressing E4orf6 did not alter the abundance of AAV circular forms but led to substantial amplification of replication form genomes. Although both E4orf6 expression and UV irradiation produced similar levels of augmentation in transgene expression from rAAV, the mechanisms of this augmentation appear to act through distinct molecular pathways.

INTRODUCTION

ADENO-ASSOCIATED VIRUS (AAV) is a single-stranded DNA virus that has been developed as a gene therapy vector. Its diverse organ tropism, capacity for integration, and nonpathogenic characteristics are several reasons why AAV is favored as a vector for gene therapy. The abundance of the membrane-associated heparin sulfate proteoglycan, which serves as a vi-

Department of Anatomy and Cell Biology and Department of Internal Medicine, University of Iowa School of Medicine, Iowa City, IA 52242.

ral receptor for AAV type 2, has been identified as one critical aspect that determines the broad range of cell types infected by recombinant AAV (rAAV) (Summerford and Samulski, 1998). Although rAAV has been demonstrated to integrate into the host genome randomly (Kearns *et al.*, 1996; Ponnazhagan *et al.*, 1997; Yang *et al.*, 1997), the ability of wild-type (wt) virus to integrate in a site-specific fashion at the AAVS1 locus on chromosome 19 (Kotin *et al.*, 1991, 1992; Samulski *et al.*, 1991) has provided an incentive to develop more targeted integration with the recombinant virus. Furthermore, persistence of rAAV in cell lines and tissues has also been associated with episomal genomes (Flotte *et al.*, 1994; Duan *et al.*, 1998a). In contrast to retroviruses, which require cell division for efficient transduction and integration (Miller *et al.*, 1990; Lewis and Emerman, 1994), the ability of rAAV to infect nondividing cells has become a salient feature promoting the use of rAAV vector in gene threapy (Alexander *et al.*, 1994; Kaplitt *et al.*, 1994; Xiao *et al.*, 1996).

Although rAAV can transduce cells in S phase, the efficiency of transduction is greatly augmented by inhibitors of DNA synthesis and topoisomerase (Russell *et al.*, 1995). Moreover, DNA-damaging agents such as ionizing radiation, UV irradiation, hydroxyurea, and cisplatinum also have been suggested to increase the transduction of stationary-phase human skin fibroblasts by AAV (Alexander *et al.*, 1994). Alternatively, the adenoviral gene product E4orf6 has also been shown to augment rAAV transduction, leading to the enhancement of AAV second-strand DNA synthesis (Ferrari *et al.*, 1996; Fisher *et al.*, 1996). In the case of E4orf6 enhancement of rAAV transduction, augmentation of AAV replication form (Rf) intermediates has suggested that this pathway may act through lytic phases of the AAV life cycle. Since adenovirus is known to be one helper virus required for wt AAV replication (Straus *et al.*, 1976; Richardson and Westphal, 1981; Berns, 1990; Ward *et al.*, 1998), lytic phase augmentation of rAAV transduction in the presence of E4orf6 is not surprising. However, helper-free limited wild-type AAV DNA synthesis has also been reported with genotoxic agents such as hydroxyurea (Yakobson *et al.*, 1987) and heat shock treatment (Yakinoglu *et al.*, 1988). Lytic-phase replication of wt AAV occurs through head-to-head and tail-to-tail replication form double-stranded DNA intermediates, which possess one covalently linked end (Richardson and Westphal, 1981; Berns, 1990; Ward *et al.*, 1998). In contrast to lytic-phase replication of AAV, latent-phase persistence of AAV has been predominantly associated with head-to-tail genomes, which can occur either as integrated proviruses (Duan *et al.*, 1997; Yang *et al.*, 1997; Wu *et al.*, 1998) or circular episomes (Duan *et al.*, 1998a). The head-to-tail orientation of AAV genomes is presently thought to occur through mechanisms of linear concatamerization or circularization of the viral genomes prior to integration. Despite the structurally unique aspects of wt AAV genomes during lytic and latent phases, little is known about the mechanisms that control these two pathways in the rAAV life cycle.

To test the hypothesis that circular intermediates are part of the AAV transduction process, an rAAV shuttle vector containing the ampicillin resistance gene and a bacterial origin of replication has been constructed in our laboratory (Duan *et al.*, 1998a). This shuttle vector was used to isolate head-to-tail circular intermediates from rAAV-infected cell lines and muscle. These circular form genomes, which occur as monomer and multimer episomes, have been associated with stable transgene expression in muscle tissue. In contrast to muscle, transduction of liver tissue with rAAV (Miao *et al.*, 1998) has been demonstrated to integrate in large head-to-tail concatemers. Although structural similarities exist for episomal and integrated rAAV genomes, it is not yet known whether episomal rAAV circular genomes represent preintegration intermediates.

Here we report that the formation of rAAV circular intermediates is augmented by UV irradiation. In contrast, adenoviral E4orf6 gene expression leads to the augmentation of Rf, but not circular, intermediates. The molecular identification of circular and replication form genomes by Southern blot suggests that these two pathways may compete in the conversion of single-stranded AAV genomes to expressible forms. Furthermore, in rAAV-infected HeLa cells and primary fibroblasts, circularized rAAV genomes are the major detectable molecular conversion event seen in the absence of any exogenous stimuli. In summary, our findings suggest that UV irradiation, but not E4orf6, enhances the normal endogenous pathways of rAAV single-stranded DNA genome conversion.

MATERIALS AND METHODS

Generation of recombinant AAV stocks

Two rAAV vectors encoding green fluorescent protein (GFP) and enhanced GRP (EGFP) transgenes were used for analysis and designated AV.GFP2ori and AV.GFP3ori (Duan *et al.*, 1998a). The cis-acting plasmid (pCisAV.GFP2ori) used for rAAV production was generated by subcloning the *Not* fragment (732 bp) of the GFP transgene from pGreenLantern (GIBCO-BRL, Gaithersburg, MD) between the cytomegalovirus (CMV) enhancer/promoter and simian virus 40 (SV40) poly(A) by blunt-end ligation. The CMV enhancer/promoter and SV40 poly(A) sequences were derived from pcDNA3.1 (Invitrogen, San Diego, CA). A 2.5-kb cassette containing β-lactamase and bacterial replication origin from pUC19 was blunt ligated downstream of the GFP reporter cassette. The inverted terminal repeat (ITR) elements were derived from pSub201 (Samulski *et al.*, 1987). The entire plasmid contains a 4.7-kbp AAV component flanked by a 2-kb stuffer sequence that was derived from the luciferase gene of pGL3-basic vector (Promega, Madison, WI). The construction of the cis-acting plasmid, pCisAV.GFP3.ori, was previously described (Duan *et al.*, 1998a). Recombinant AAV stocks were generated by cotransfection of pCisAV.GFP3ori and pRep/Cap (Fisher *et al.*, 1996) together with coinfection of recombinant Ad.CMVlacZ (Fisher *et al.*, 1996) in 293 cells. The rAV.GFP3ori virus was subsequently purified through three rounds of CsCl banding followed by heat inactivation of adenovirus at 60°C for 1 hr as previously described (Duan *et al.*, 1997). DNA titers were determined by viral DNA slot-blot hybridization against GFP or EGFP ^{32}P-labeled probe with copy number plasmid standards. The absence of helper adenovirus was confirmed by histochemical staining of rAAV-infected 293 cells for β-galactosidase, and no recombinant adenovirus was found in 10^{10} particles of purified rAAV stocks. The absence of wt AAV in recombinant stocks was confirmed using previously described methodologies (Duan *et al.*, 1997) with a sen-

sitivity of less than 1 functional wt AAV particle per 10^{10} recombinant DNA particles.

UV irradiation, AAV infection, and FACS analysis

FF cells (fetal fibroblasts) were prepared in our laboratory from 13-day fetal ferret embryos. Cells were maintained in Dulbecco's modified Eagle's medium (DMEM) supplemented with 10% fetal calf serum (FCS) and a 1% penicillin–streptomycin mixture. Cells were plated the day before infection at a density of 1×10^6 cells per 60-mm plate. The following day, confluent monolayers were washed with phosphate-buffered saline (PBS) and immediately irradiated using a Stratalinker UV crosslinker (Stratagene, La Jolla, CA) at different doses of UV. Cells remained exposed to air during irradiation procedures. Immediately after irradiation, cells were infected with AV.GFP2ori virus at a multiplicity of infection (MOI) of 100 DNA particles per cell. Infection was carried out in DMEM with 2% FCS for 2 hr. Following infection, the level of FCS was increased to 10% (v/v) final concentration to prevent serum deprivation. Cells were then incubated at 37°C for an additional 48 hr. At the termination of the experiment, cells were washed with PBS, trypsinized, and analyzed by fluorescence-activated cell sorting (FACS) to determine the percentage of GFP-positive cells.

Isolation of AAV circular intermediates

Hirt DNAs were isolated according to modications of previously described protocols (Hirt, 1967; Duan *et al*., 1998a). In brief, cells were trypsinized, pelleted, and stored at −80°C prior to the Hirt procedure. Cells were resuspended in 320 μl of Hirt extraction buffer containing 10 m*M* Tris and 10 m*M* EDTA, pH 8.0. One microliter of DNase-free RNase (10 mg/ml) and 36 μl of 10% sodium dodecyl sulfate (SDS) were added to samples and cells were incubated at 37°C for 0.5 hr. Samples were further treated with pronase (1 mg/ml) and proteinase K (20 μg/ml) for 2 hr at 37°C. After addition of NaCl to a final concentration of 1.1 *M*, samples were incubated at 4°C overnight. Samples were then centrifuged for 30 min at 4°C, and the supernatant was removed and extracted with phenol–chloroform and precipitated in 100% ethanol in the presence of 1 μl of yeast tRNA (10 mg/ml) overnight at −20°C. After centrifugation for 30 min, pellets were washed with 70% ethanol and the pellet dried and resuspended in 50 μl of water. After determining the concentrations of DNA by OD_{260}, 3 μl of Hirt DNA (out of 50 μl) was transformed into *Escherichia coli* SURE cells ($>1 \times 10^9$ CFU/μg; Stratagene) by electroporation. The total number of bacterial colonies was quantitated for each experimental condition. The structure of rescued AAV circular intermediate plasmids was analyzed by restriction analysis and Southern blotting. Briefly, the predominant diagnostic restriction digest for head-to-tail circular intermediates included liberation of a 300-bp ITR array following digestion with *Sph*I. Other diagnostic digests included *Pst*I and *Ase*I, which cut twice and once within circular form genomes, respectively. Southern blots were performed using ITR and GFP or EGFP ^{32}P-labeled DNA.

Hirt DNA Southern blot analysis of circular and replication form genomes.

Hirt DNA samples (10 μl of the 50 μl total Hirt, which corresponds to Hirt DNA from 4×10^5 cells) were digested in a 20-μl total reaction volume using different restriction enzymes (*Ase*I, *Pst*I, and *Sph*I). Mock Hirt digestions under identical reaction conditions but in the absence of enzyme were also performed as controls. After 3 hr of digestion the entire sample was run in an 8% agarose gel for Southern blotting or 5 μl of the samples out of 20 μl was transformed into *E. coli* to determine total rescued colony-forming units.

RESULTS

UV induces augmentation of rAAV gene expression

To evaluate the mechanisms of UV-mediated augmentation in rAAV transduction, we utilized primary fetal fibroblasts derived from 13-day (E13) ferret embryos. As previously demonstrated in primary fibroblasts (Alexander *et al*., 1994), UV doses ranging from 15 to 50 J/m^2 resulted in significant dose-dependent enhancement of rAAV GFP gene expression as detected by FACS analysis (Fig. 1). Maximal enhancement (54-fold) in the number of transgene expressing cells was seen at 50 J/m^2 UV when an AAV MOI of 100 DNA particles/cell was used. In addition, increases in the mean fluorescence intensity were also detected at UV doses of 25 and 50 J/m^2. Given the apparent increase in the intensity of transgene expression following UV irradiation, we sought to rule out that augmentation occurred primarily at the transcriptional level of the CMV promoter driving GFP expression in our rAAV construct.

To test this hypothesis, HeLa cells were transfected with 100 ng of pCisAV.GFP2ori plasmid and UV irradiated on the following day of transfection. We expected that if UV irradiation induced cellular factors responsible for increased expression from our CMV transgene cassette, we would observe an augmentation in transgene expression from the transfected proviral plasmid. Doses of UV irradiation ranging from 15 to 50 J/m^2 did not increase the percentage of cells expressing GFP (Fig. 1C). However, the relative mean fluorescence intensity of positive cells increased 1.9-fold at 25 J/m^2 UV and by 2.7-fold at 50 J/m^2 UV. This enhancement in the mean fluorescence intensity of cells was similar to that seen following rAAV transduction (compare Fig. 1B and C). These data suggest that despite the apparent UV transcriptional induction (maximal, 2.5-fold) of our rAAV transgene cassette, this mechanism is insufficient to explain enhancement of rAAV transduction by UV (54-fold maximum at 50 J/m^2 UV) as determined by the percentage of positive cells. However, since transfection preceded UV irradiation, it remained possible that UV irradiation damage to the pCisAV.GFP2ori plasmid rendered the plasmid less transcriptionally active. To rule out this possibility, the order of UV irradiation and transfection was reversed (data not shown). These experimental results mirror those shown in Fig. 1C and demonstrated a slight enhancement in mean fluorescence intensity of cells in the absence of increased transgene-expressing cell numbers. Given the fact that transcriptional effects appear not to be the sole reason for UV-mediated augmentation of rAAV transduction, we sought to evaluate other molecular end points that might delineate the molecular events involved in this augmentation.

UV irradiation enhances the formation of AAV circular intermediates

Several pathways have been previously suggested as end points for the molecular conversion of AAV genomes following infection of cell lines and tissues. These include both AAV replication form (Rf monomers [Rf_m] and Rf dimers [Rf_d]) (Ferrari *et al*., 1996; Fisher *et al*., 1996) and AAV circular intermediates (Duan *et al*., 1998a). Specifically, Rf_m and Rf_d have been shown to increase in the presence of the adenoviral protein E4orf6. In contrast, circular intermediates have been associated with long-term persistence of AAV genomes in muscle. Although these molecular end points are incapable of delineating mechanisms of transduction and augmentation by environmental stimuli, we reasoned that pathways that augment replication form intermediates (which include characteristic head-to-head and tail-to-tail genomes) may be distinct from those that are responsible for circular intermediate formation (which include characteristic head-to-tail monomer and concatemer AAV genomes). To test this hypothesis, we characterized the abundance of both replication form and circular intermediates following rAAV transduction of FF cells and HeLa cells.

Circular intermediates were quantified using two shuttle vectors, AV.GFP2ori and AV.GFP3ori, which both encode the ampicillin resistance gene and bacterial replication origin. AAV circular intermediates were recovered from rAAV-infected FF cells using the Hirt DNA isolation procedure followed by transfection of Hirt DNA into *E. coli* Sure cells. The predominant forms of circular intermediates seen following UV irradiation and rAAV infection were similar to those reported for muscle and involved head-to-tail circularized genomes. Southern blot analysis of rescued circular intermediates, using GFP and ITR fragments as probes (Fig. 2A), demonstrate an extremely uniform structure as shown in Fig. 2B. Restriction enzyme analysis using enzyme cutters that cleave once in the AAV genome gave rise to a 4.7-kb linear fragment indicative of monomer genomes. Futhermore, *Sph*I digestion liberated an approximately 300-bp fragment characteristic of a partial head-to-tail ITR array. Dideoxy sequence analysis using primers nested outside the ITR confirmed the orientation of these ITR arrays but was incapable of determining whether deletions had occurred in the central region of the ITR junction (data not shown). We have completed a more detailed structural characterization of ITR arrays within circular AAV genomes by chemical sequencing (Duan *et al*., 1999). Results from these studies suggest that the predominant structural form of rAAV circular genomes has one intact ITR flanked by two D sequences. This structure is reminiscent of the previously reported double-D AAV plasmid (Xiao *et al*., 1997). Other forms with more than one complete ITR flanked by two D sequences were also seen and may reflect a continuous conversion process to a more stable form. The implications of these structural studies suggest mechanisms by which recombination occurs within ITRs of stem–loop annealed single-stranded AAV genomes to give circular monomers (Duan *et al*., 1999).

The abundance of this primary molecular form of circular intermediates was quantitated following UV irradiation. As shown in Fig. 2C, the number of rescued clones from Hirt DNA of rAAV-infected cells increased in a dose-dependent fashion from 5 to 15 J/m^2. At higher levels of UV irradiation (50 J/m^2) the number of rescued plasmid clones decreased. However, when the structural characteristics of isolated rescued plasmids were analyzed by Southern blot, the percentage of head-to-tail circular form genomes (as shown in Fig. 2B) increased linearly over all doses of UV irradiation (ranging from 22% at 0 J/m^2 to 88% at 50 J/m^2). The total abundance of head-to-tail circular intermediates increased 15-fold between 0 and 25 J/m^2. We hypothesize that the decrease in total rescued clones between 25 and 50 J/m^2 reflects an overall decrease in cell viability. However, given the linear increase in the specific structure of circular intermediates, we anticipate that molecular events augmented by UV irradiation lead to a dose-dependent increase in the abundance of head-to-tail circularized rAAV genomes.

Adenovirus E4 gene expression augments rAAV transduction through pathways distinct from circular intermediate formation

To compare molecular pathways augmented by E4orf6 expression and UV irradiation, we directly evaluated the extent of circular and Rf intermediate formation in fetal ferret fibroblast cells (FF cells). Confluent monolayer of FF cells were coinfected with AV.GFP2ori (MOI of 100 DNA particles/cell) and increasing doses of replication-defective (E2-deleted) adenovirus (Ad.dl802). This recombinant virus is capable of expressing high levels of E4orf6 in the absence of viral replication. As previously reported, our results confirmed the ability of Ad.dl802 to augment rAAV transgene expression more than 100-fold at high MOIs (Fig. 3A and B). However, this augmentation in transgene expression by rAAV was not accompanied by alterations in the abundance of circular intermediate formation (Fig. 3C). The abundance of Southern blot-confirmed circular clones with head-to-tail ITR retrieved at all doses of Ad.dl802 infection was similar to that seen in unirradiated cells of UV experiments. Furthermore, in contrast to UV irradiation, the total abundance of rescued CFU isolated from Hirt DNA (regardless of their structural characteristics) did not change over all doses of adenovirus.

Because assays for circular intermediates utilized an indirect rescue approach in bacteria, we sought to determine whether structural confirmation of these circular form AAV genomes could be obtained directly from Southern blots of Hirt DNA. Hirt Southern blots were used to compare directly the molecular conversion of rAAV single-stranded DNA (ssDNA) genomes following both UV and E4orf6 augmentation. Figure 4 depicts a representative Hirt Southern blot of AV.GFP2ori-infected primary FF cells (at an MOI of 500) probed with GFP. Initial attempts to evaluate Hirt Southern blots from rAAV-infected FF cells and HeLa cells were unsuccessful in visualizing circular form genomes at MOIs of 100 particles/cell. Hence the higher MOIs were necessary for these studies. However, at these MOIs the induction of transgene expression by UV and Ad infection quickly approached saturation at 100% (data not shown). Nonetheless, an indirect comparison between molecular forms of AAV, at MOIs of 500 particles/cell, and the induction of GFP transgene expression cells, at MOIs of 100 particles/cell, can be made for each of the experimental conditions. For example, at maximal levels of circular intermediate formation (25 J/m^2) 24% of fibroblasts express GFP. Moreover,

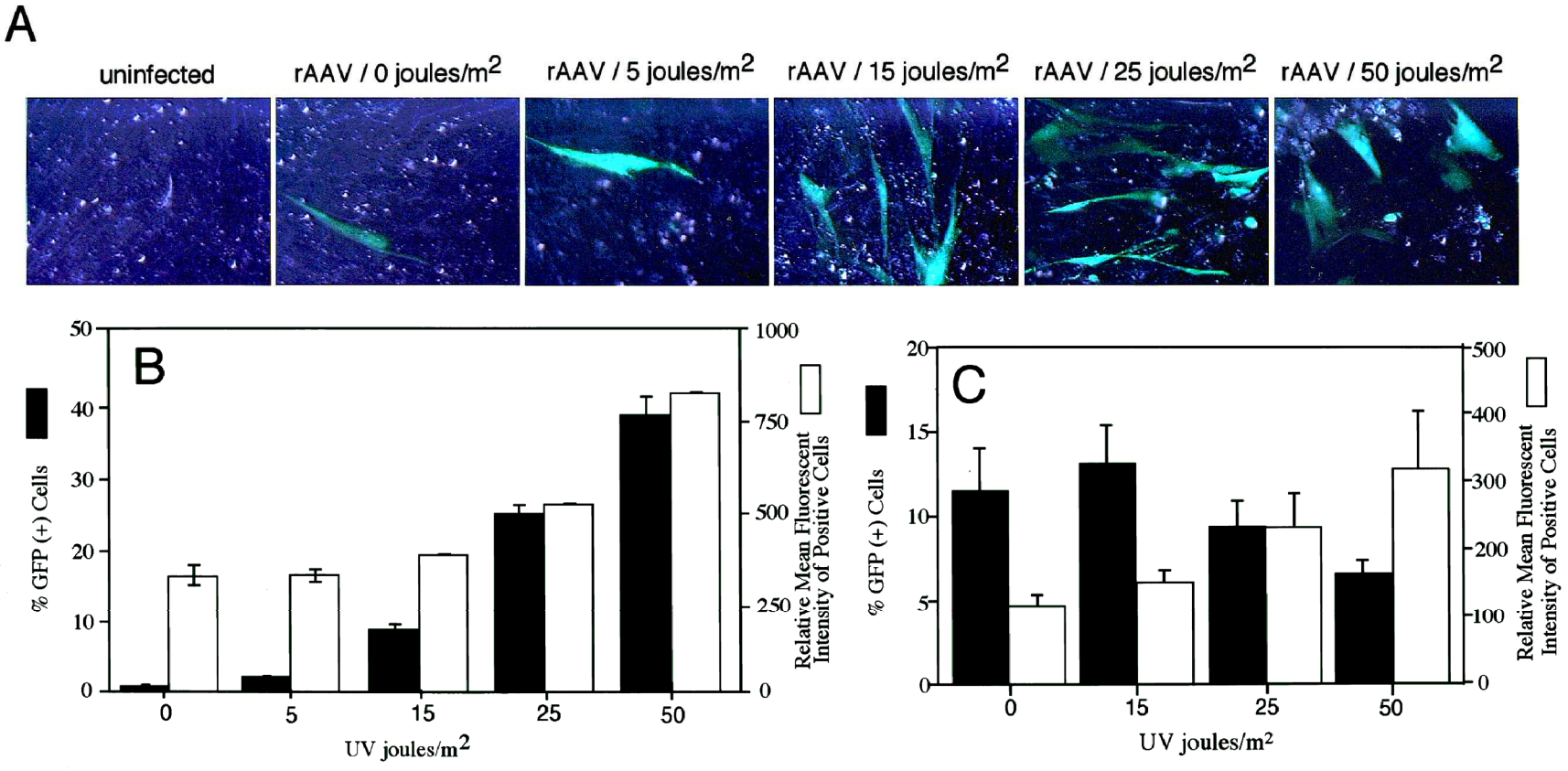

FIG. 1. Induction of rAAV transgene expression by UV irradiation. Confluent monolayers of FF cells were infected with AV.GFPori2 virus (MOI of 100 DNA particles/cell) following UV irradiation at the indicated doses. Representative photomicrographs demonstrating the induction of transgene expression at 48 hr following UV irradiation are given in **(A)**. The percentage (black bars) and mean fluorescence intensity (white bars) of GFP-expressing cells were quantitated by FACS analysis at 40 hr postinfection **(B)**. Data represent the means (±SEM) of three independent experiments ($N = 5$). The transcriptional effect of UV irradiation on the CMV promoter from the pCisAV.GFP2ori plasmid was evaluated by transient transfection assays **(C)**. In these studies 5×10^5 HeLa cells were plated on 35-mm plates and transfected with liposome:DNA complexes containing 100 ng of pCisAV.GFP2ori plasmid on the following day postplating, using standard manufacturer procedures for LipofectAMINE-mediated transfection (GIBCO-BRL). Cells were UV irradiated at the indicated doses 24 hr after the transfection. The percentage of GFP-expressing cells (black bars) and relative mean fluorescence intensity of positive cells (white bars) were determined by FACS analysis 48 hr following transfection. Data represent the mean (±SEM) of at least three independent transfections for each experimental data point.

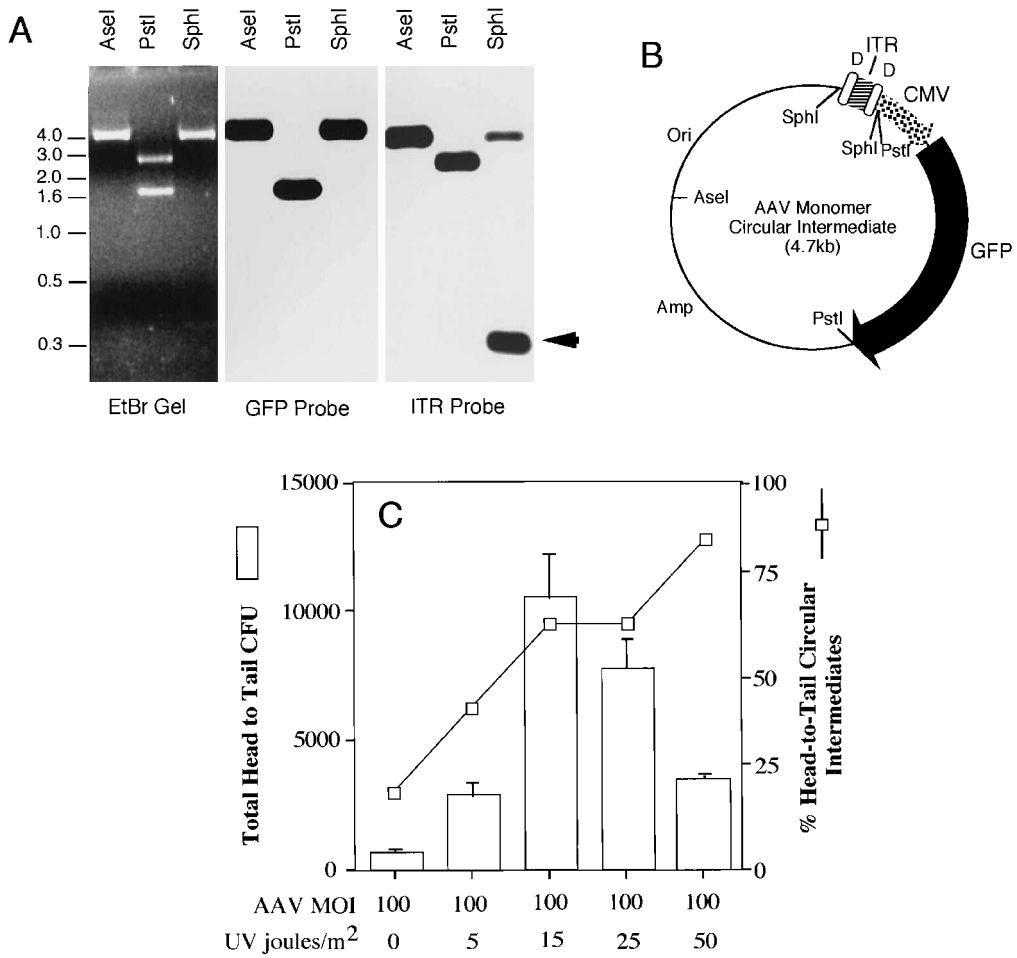

FIG. 2. UV irradiation increases the abundance of AAV circular intermediates. The AV.GFP2ori shuttle vector was used to rescue circular intermediates at 40 hr following transduction of FF cells by bacterial transformation of Hirt DNA. Restriction enzyme analysis of a typical rescued circular intermediate is given in **(A)** with molecular weights (kb) shown on the left. The ethidium-stained agarose gel prior to Southern blotting is shown on the left of **(A)**. Southern blot filters of this gel were hybridized with GFP (middle) or ITR (right) ^{32}P-labeled probes. *Ase*I digestion (which cuts once in the viral genome) linearizes the provirus, giving rise to a 4.7-kb band. *Pst*I digestion (which cuts twice in the viral genome) excises a 1.7-kb fragment, which hybridizes to the GFP probe. *Sph*I digestion releases a 300-bp ITR array (marked by an arrowhead). A graphic representation of the predominant form of circular intermediates isolated from FF cells is given in **(B)**. **(C)** depicts the effects of UV irradiation on the abundance of AAV circular intermediates in FF cells. Confluent monolayers of FF cells were UV irradiated at different doses (5, 15, 25, and 50) J/m^2) prior to infection with AV.GFP2ori virus at an MOI of 100 DNA particles/cell. Hirt DNA was isolated from an equal number of cells (2×10^6) for each condition at 40 hr postinfection and a portion of this DNA (3 μl out of a total of 50 μl) was used to transform *E. coli* Sure cells. Bars indicate the total number of head-to-tail CFU isolated from a 60-mm plate. Values indicate the means (±SEM) of six independent data points for each condition. The percentages of total recovered CFU that had Southern blot-determined head-to-tail circular form genomes [as shown in **(A)** and **(B)**] are indicated by the overlaid line in this graph. These data were generated by Southern blotting of nine colonies for each experimental data point.

comparison of UV-irradiated Hirt DNA at 25 J/m^2 to Ad.dl802-infected cells at an MOI of 100 to 1000 particles/cell gave similar extents of augmentation in transgene expression but distinctly different molecular forms of AAV genomes.

As previously demonstrated, Ad.dl802 infection at these doses significantly increased Rf_m and Rf_d formation in a dose-dependent manner (Fig. 4). Little enhancement in the replication form genomes of AAV was seen when cells were irradiated at increasing doses of UV. Under these conditions, Hirt DNA from AV.GFP2ori-infected FF cells gave rise to a faint band that migrated at approximately 2.8 kb, consistent with the molecular weight of supercoiled rescued head-to-tail circular form plasmids. This band was not present in mock Hirt DNA spiked with rAAV (Fig. 4, lane 1) and hence did not represent a molecular form of single-stranded or duplex form linear DNA. Following UV irradiation at different doses (5, 15, and 25 J/m^2), this putative circular form AAV genome demonstrated a clear increase in intensity that correlated with augmentation in rescued circular intermediates in bacteria from the same Hirt DNA samples (Fig. 4, lanes 3, 4, and 5). No enhancement in the intensity of this candidate circular form was seen in Hirt Southern blots of cells infected with increasing doses of Ad.dl802

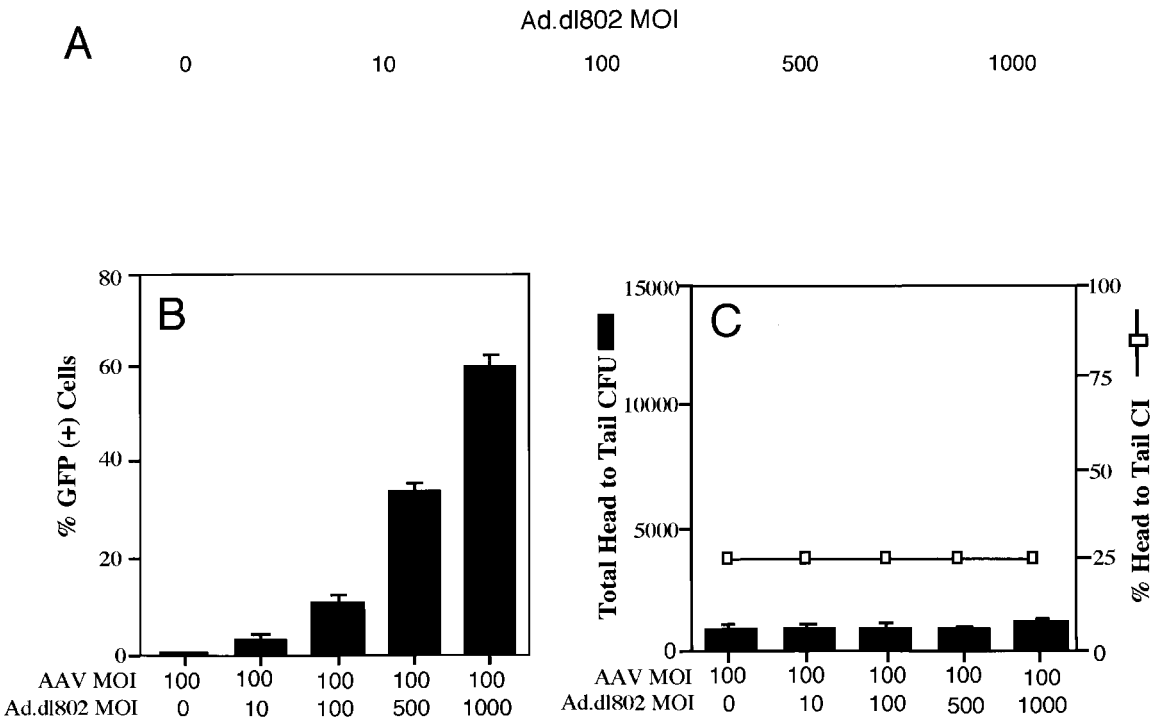

FIG. 3. Replication-defective adenovirus expressing E4orf6 augments rAAV transduction in the absence of an increased abundance of AAV circular intermediates. Confluent monolayers of FF cells were coinfected with AV.GFP2ori virus (MOI of 100 DNA particles/cell) and increasing doses of Ad.dl802. **(A)** depicts representative fluorescence photomicrographs demonstrating E4-mediated augmentation of rAAV transduction. The percentage of cells expressing GFP were determined by FACS analysis at 40 hr following coinfection of cells **(B)**. This graph depicts the mean (±SEM) of two independent assays performed in triplicate ($N = 6$). Hirt DNA was isolated from an equal number of cells (2×10^6) for each condition 40 hr postinfection and a portion of this DNA (3 μl out of a total of 50 μl) was used to transform *E. coli* Sure cells **(C)**. Solid bars indicate the total number of head-to-tail CFU isolated from a 60-mm plate. Values indicate the mean (±SEM) of six independent data points for each condition. The percentages of total recovered CFU that had Southern blot-determined head-to-tail circular form genomes [as shown in **(A)** and **(B)**] are indicated by the overlaid line in this graph. These data were generated by Southern blotting of nine colonies for each experimental data point.

(Fig. 4, compare lanes 7–10). This lack of an increase correlated with unchanged levels in the abundance of rescued plasmids from the same Hirt samples (Fig. 4). In both UV and Ad coinfection experiments there was a slight increase in the amount of AAV ssDNA, which correlated with the level of augmentation in transgene expression and the extent of environmental stimuli provided. The reason for this increase is unclear but may reflect increased uptake of virus. Despite this, only UV irradiation enhanced the abundance of this candidate circular form AAV intermediates.

AAV circular intermediates augmented by UV appear to be supercoiled

To confirm that this candidate band migrating at 2.8 kb induced by UV treatment was indeed circular form genomes, we performed restriction enzyme analysis of Hirt DNA using *Ase*I and *Pst*I (Fig. 5A). We anticipated that if this form was circular, *Ase*I, which cuts once within the viral genome, would give rise to a linear 4.7-kb GFP hybridizing fragment. In contrast, *Pst*I, which has two sites in the rAAV genome flanking the CMV.GFP transgene, should give rise to a 1.7-kb GFP hybridizing fragment. As shown in Fig. 5A, both *Ase*I and *Pst*I digestion of Hirt DNA are consistent with this band representing a circular form of the AAV genome. In addition, digestion of Hirt DNA with *Ase*I, prior to transformation of bacteria, completely eliminated rescued circular intermediates (Fig. 5B). These results confirm previous findings that demonstrate that linear double-stranded AAV genomes harboring an *amp* and an *ori* are not capable of yielding replication-competent plasmids following transformation of bacteria (Duan *et al.*, 1998a). In summary, these data provide direct evidence for the existence of circular form AAV genomes prior to transformation in bacteria. Given the apparent molecular weight and comigration of these circular form genomes with supercoiled rescued circular form genomes in bacteria (Fig. 5), we speculate that circular AAV genomes also exist as supercoiled molecules *in vivo*. Therefore we have concluded that AAV circular intermediates exist as supercoiled, double-stranded, and closed circular forms prior to entry into bacteria, and that the abundance of AAV circular intermediates is increased on UV irradiation. Furthermore, the replication form monomer and dimers were not significantly

augmented by UV irradiation. These results suggest that UV induces cellular permissiveness that favors the formation of AAV circular intermediates. Although UV-mediated augmentation of rAAV tranduction appears to occur through alternative pathways than that in the presence of adenoviral E4orf6, at high doses of UV irradiation a minor band consistent with Rf dimers was also observed (Fig. 4). This may represent a conversion to lytic pathways at high does of UV and suggests that UV augmentation of rAAV transduction may be complex.

Induction of circular intermediates by UV is not limited to fetal fibroblasts but also occurs in HeLa cells

To test whether the effects of UV-augmented abundance in circular AAV genomes were specific to fibroblasts, we performed similar studies in HeLa cells. As shown in Fig. 6A, rAAV transduction is also augmented by UV in HeLa cells. In these studies, HeLa cells were infected with increasing doses

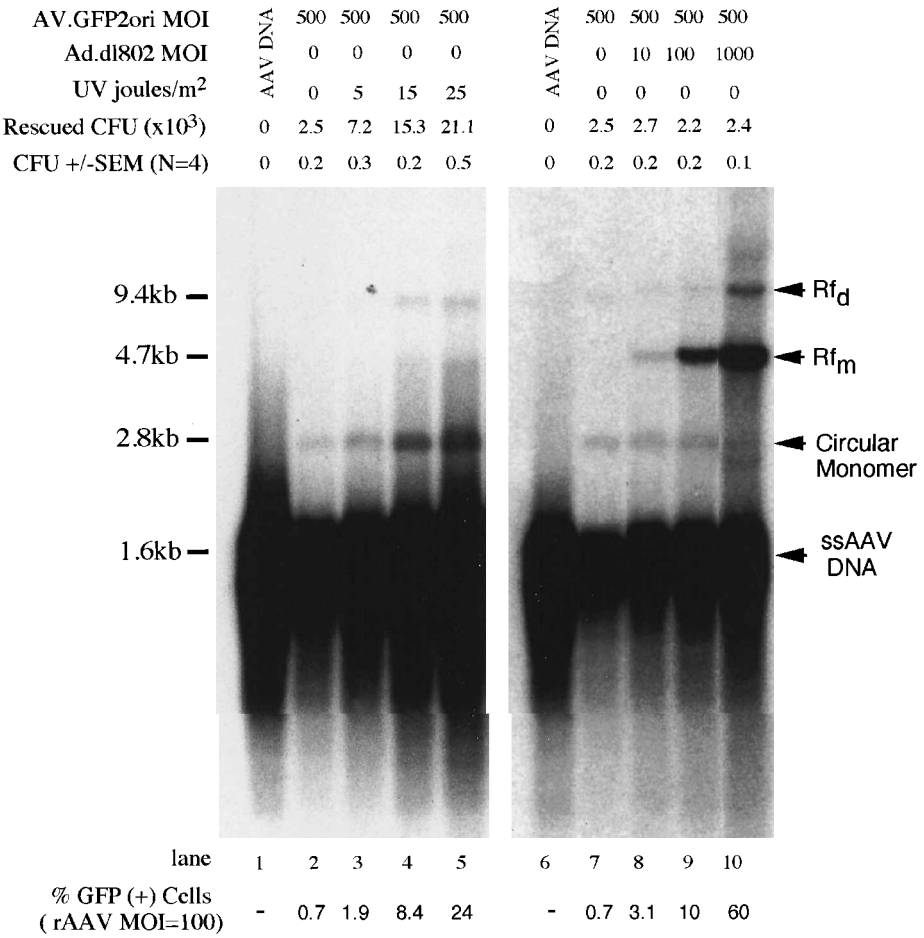

FIG. 4. Hirt DNA analysis of circular and replication form genomes by Southern blotting. Southern blot analysis of Hirt DNA isolated from AV.GFP2ori-infected FF cells (MOI of 500 DNA particles/cell) following UV irradiation (lanes 1–5) or coinfection with increasing doses of Ad.dl802 virus (lanes 6–10) is shown. Hirt DNA samples were prepared 24 hr following infection from 2×10^6 cells. Equal amounts of Hirt DNA (10 μl out of a 50-μl Hirt preparation) were loaded onto a 0.8% agarose gel. Gels were transferred to nylon membranes and the filters probed with a ^{32}P-labeled 1.7-kb *Pst*I GFP fragment isolated from pcisAV.GFP2ori. Lanes 1 and 6 represent controls for AAV DNA alone, which were generated by spiking an equivalent amount of rAAV virus, as used for infections, into mock cell lysates prior to Hirt purification. Rescued replication-competent plasmids from Hirt DNA (CFU) were determined by transforming 3 μl of each Hirt sample (out of 50 μl) into *E. coli*. The CFU values above each lane depict mean values ($\pm$SEM) for $N = 4$ independent infections at an rAAV MOI of 500 DNA particles/cell. The DNA samples shown in this Southern were included in the CFU analysis. Single-stranded AAV DNA, Rf_m, Rf_d, and candidate circular from genomes are marked to the right of the gel. Molecular weights (in kb) are given to the left of the gel. The band indicating putative circular form genomes was not visible at MOIs equal to 100 DNA particles/cell (data not shown). Hence MOIs of 500 DNA particles/cell were used for these studies. Since transgene expression at this MOI is outside the linear range to assess induction by UV and Ad.dl802, comparative values for the extent of transgene induction are given at MOIs of 100 DNA particles/cell below each lane.

of AV.GFP3ori virus (Fig. 6A). Maximal induction (10-fold) was seen at MOIs of 15–50 particles/cell. At high MOIs of 500 DNA particles/cell, transgene expression was saturated even in the absence of UV irradiation. As seen in Fig. 6B, UV irradiation augmented the abundance of bacterial rescued head-to-tail AAV circular intermediates, while coinfection with Ad.dl802 led to a 30% decrease in the abundance of these circular forms. To compare directly the abundance of bacterial rescued circular AAV genomes to identifiable circular form molecules in Hirt DNA, Southern blot analysis was performed on the identical samples analyzed in Fig. 6B. As seen in Fig. 6C, transformation rescue assays demonstrated a correlation between the abundance of circular form genomes detected by Southern blot. Furthermore, there was a decrease in the abundance of AAV circular intermediates after infection with Ad.dl802 at an MOI of 1000 (Fig. 6C, lane 5). As seen in fibroblasts, HeLa cell Hirt digestion with *Ase*I and *Pst*I gave Southern blot restriction patterns consistent with this 2.8-kb band being a supercoiled circular form of the AAV genome (data not shown). In addition, *Ase*I digest of the both UV-irradiated and unirradiated Hirt DNA samples prior to transformation of bacteria led to the complete ablation of rescued CFU (data not shown). In summary, we provide in two independent cell types evidence suggesting that the augmentation of rAAV transduction by UV and E4orf6 occurs through pathways that lead to two distinct molecular conversion events of the single-stranded AAV genome.

DISCUSSION

Although rAAV can transduce a wide range of cell types (McCown *et al.*, 1996; Xiao *et al.*, 1996; Clark *et al.*, 1997; Koeberl *et al.*, 1997; Lynch *et al.*, 1997; Chamberlin *et al.*, 1998), little is known about what aspects of transduction make this vector efficient for some organs and less so for others. Nu-

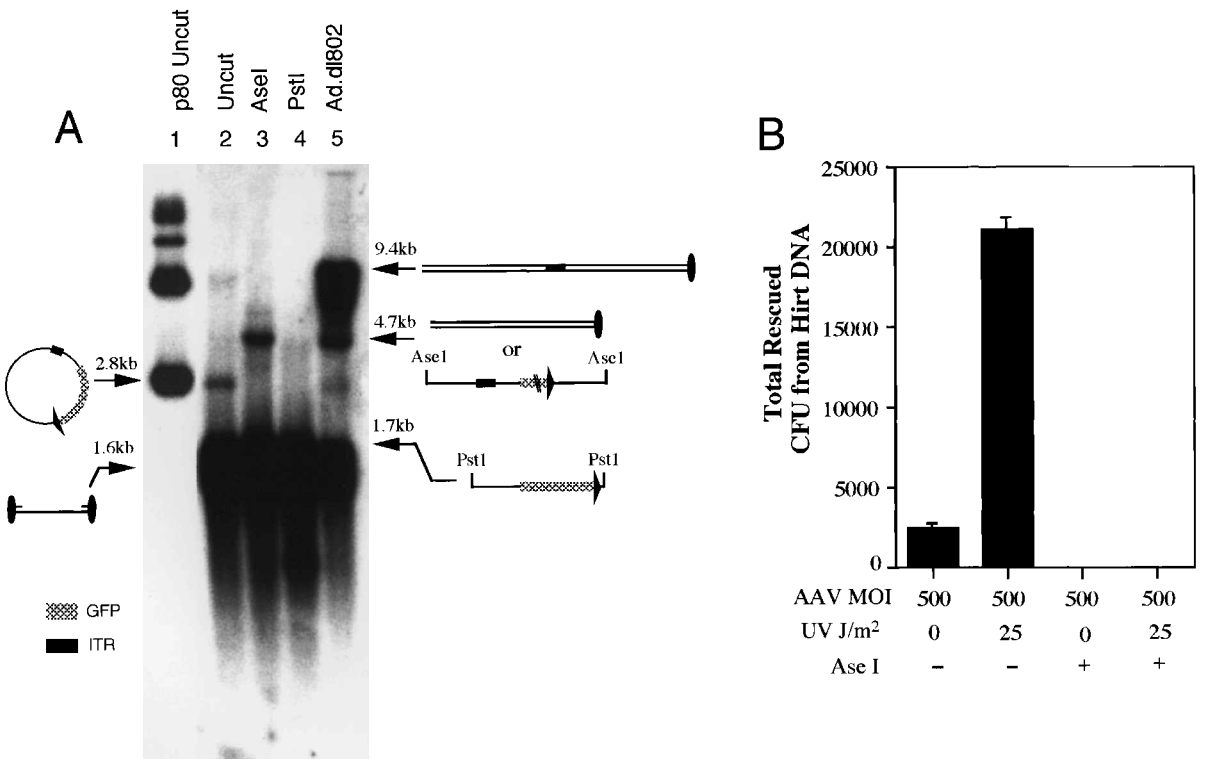

FIG. 5. Structural confirmation of rAAV circular intermediates in Hirt DNA by Southern blotting. Restriction enzyme analysis of Hirt DNA isolated from AV.GFP2ori-infected FF cells was used to confirm the circular structure of 2.8-kb GFP-hybridizing bands on Southern blot **(A)**. Hirt DNA samples were prepared 24 hr following infection with AV.GFP2ori virus (MOI of 500 DNA particles/cell). For comparison with Rf intermediates, cells coinfected with Ad.dl802 virus (MOI of 1000 DNA particles/cell) were also analyzed (lane 5). One-fifth portions of a 60-mm plate of Hirt DNA sample (10 μl) were digested in a total volume of 20 μl with different restriction enzymes (uncut, *Ase*I, *Pst*I) prior to Southern blotting and hybridization against GFP ^{32}P-labeled probes (1×10^7 CPM/ml) (lanes 2–4). An undigested, bacterial rescued circular intermediate plasmid (p80, as shown in Fig. 2B) was also run as a positive control for the migration of supercoiled circular form rAAV genomes (lane 1). The structure and molecular weight of GFP-hybridizing bands are shown to the left and right of the Southern blot. In studies using *Ase*I digestions conditions as shown in the Southern blots, 5 μl out of a 20-μl digestion reaction was transformed into *E. coli* to assess the abundance of replication-competent plasmids (CFU) in Hirt DNA from rAAV-infected FF cells **(B)**. Mock digestions were also performed under identical buffer condition but in the absence of *Ase*I enzyme to control for nonspecific degradation of viral DNA during digestion procedures. These data represent the mean total CFU (±SEM) rescued from four independent data points for each condition.

merous barriers to efficient rAAV transduction may exist, including (1) the abundance of surface receptor(s), (2) the efficiency of endocytosis, (3) the efficiency of nuclear trafficking and viral uncoating in the nucleus, (4) the molecular conversion of single-stranded AAV genomes to expressible forms, and (5) the stability of the transformed double-stranded genomes. In the present study, we have attempted to define further the molecular conversion events that control the transformation of single-stranded AAV genomes to expressible forms. Given the low efficiency of rAAV transduction in cell types such as the lung, a better understanding of pathways that can lead to augmentation in the molecular conversion of ssDNA viral genomes to expressible forms is highly relevant to gene therapy.

It is generally thought that many environmental stimuli such as UV, DNA synthesis inhibitors, and E4orf6 expression augment rAAV transduction by inducing cellular factors that facilitate the molecular transformation of single-stranded AAV genomes. Adenovirus E4orf6 expression has been demonstrated to increase the abundance of replication form AAV intermediates associated with the lytic replication phases of AAV. Although little is known about the mechanisms that control this effect, it is generally accepted that adenovirus-mediated AAV transduction of cells normally is associated with lytic replication of AAV, leading to head-to-head and tail-to-tail genomes. UV irradiation is also capable of augmenting rAAV transduction. Although it has been previously proposed to act through similar pathways leading to the augmentation of Rf genomes (Ferrari *et al.*, 1996), one report has suggested that augmentation of endocytic pathways of viral uptake may be involved in UV-mediated AAV transduction (Duan *et al.*, 1998b). Our data,

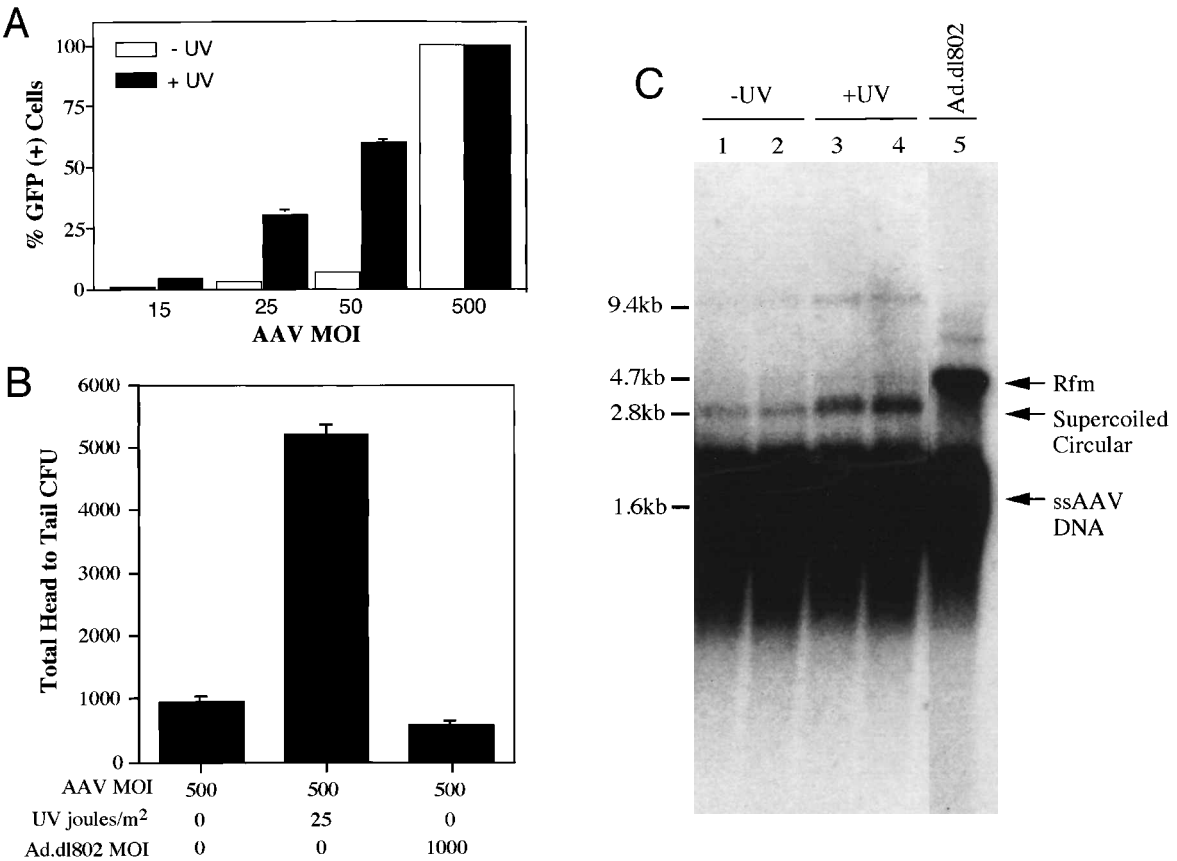

FIG. 6. UV irradiation but not E4 expression augments the abundance of circular intermediates in HeLa cells. Confluent monolayers of HeLa cells were infected with increasing doses of AV.GFP3ori virus (MOIs of 15, 25, 50, and 500 DNA particles/cell) immediately following UV irradiation at 25 J/m^2. GFP expression was evaluated by FACS analysis 24 hr following the infection **(A)**. Data represent the mean (±SEM) of six independent data points for each experimental condition. Hirt DNA was also isolated 24 hr postinfection with AV.GFP3ori virus (MOI of 500 particles/cell) and 3 μl of this sample (out of a total of 50 μl) transformed into *E. coli* Sure cells. The abundance of head-to-tail circular intermediates within rescued plasmid clones was quantitated following Southern blot analysis for both UV-irradiated and Ad.dl802 coinfected cultures **(B)**. These data depict the mean (±SEM) of eight independent data points for each experimental condition. The same Hirt samples were used in Southern blotting analysis to determine the abundance of AAV circular form genomes following either UV treatment or Ad.dl802 coinfection **(C)**. Lanes 1 and 2 represent HeLa cells infected with AAV alone in the absence of UV. In contrast, cells infected with rAAV following UV irradiation at 25 J/m^2 (lanes 3 and 4) and coinfection with Ad.dl802 at an MOI of 1000 particles/cell (lane 5) are also shown. Molecular weights are given to the left of the Southern blot and arrows mark the positions of Rf_m, supercoiled circular, and single-stranded DNA forms of the rAAV genome.

which demonstrate that UV irradiation leads to increased abundance of circular AAV genomes, suggest that this pathway of augmentation may be distinct from that in the presence of adenoviral E4orf6. Direct comparison of molecular forms of rAAV genomes on Hirt Southern blots confirmed that replication form-enhanced second-strand synthesis by E4orf6 is distinct from that of UV augmentation of circular form AAV genomes. Furthermore, in HeLa cells, the decrease in the abundance of circular form genomes in the presence E4orf6 expression suggests that these two pathways may compete in the transformation of single-stranded AAV genomes.

Given the fact that circular form genomes, and not replication form genomes, are the most abundant conversion product in cells infected with rAAV alone, we hypothesize that circular intermediate formation may represent the normal latent endogenous pathway of transformation in the absence of external stimuli. Our results in fibroblasts, which demonstrate an increase in both single-stranded DNA and circular form genomes, are consistent with previous reports suggesting increased endocytic processing of virus following UV (Duan *et al*., 1998b). Hence, under these conditions, the molar increase in rAAV genomes following UV may lead to the enhancement of already existing pathways for circular intermediate formation. In contrast, data on HeLa cells, which demonstrate increased circular form genomes in Hirt Southern blots, in the absence of increased single-stranded DNA, suggest that other pathways that may directly alter the efficiency of genome conversion to circular forms may be augmented. Such pathways may involve DNA repair enzymes such as ligases and recombination enzymes needed for the molecular conversion events involved in circular intermediate formation.

In summary, the enhancement of rAAV transduction by UV and E4orf6 correlates with the induction of two distinct molecular genomes conversion pathways. Despite this correlation, functional differences between these two forms of rAAV intermediates (circular or replicative forms) are not well understood. For example, it is presently unclear whether both of these types of intermediates have similar capacities for integration and/or long-term episomal persistence. Augmentation of these pathways may help in the design of new strategies for increasing the efficacy of rAAV in gene therapy approaches. Given the evidence that circular intermediates convey increased persistence to rAAV genomes in muscle long term, strategies to augment these intermediates may prove extremely efficacious for other organs. By understanding the mechanisms of UV-augmented AAV circular intermediate formation, more suitable methods for *in vivo* use can be developed to increase the efficacy of rAAV-mediated gene therapy.

ACKNOWLEDGMENTS

We gratefully acknowledge Dr. Terry Ritchie for expert editorial assistance in the preparation of the manuscript. This work was supported by NIH R01 DK/HL58340 (J.F.E.). We also thank Gene Hess and Justin Fishbaugh for help during the FACS analysis at the University of Iowa Flow Cytometry Facility.

REFERENCES

ALEXANDER, I.E., RUSSELL, D.W., and MILLER, A.D. (1994). DNA-damaging agents greatly increase the transduction of nondividing cells by adeno-associated virus vectors. J. Virol. **68,** 8282–8287.

BERNS, K.I. (1990). Parvovirus replication. Microbiol. Rev. **54,** 316–329.

CHAMBERLIN, N.L., DU, B., DE LACALLE, S., and SAPER, C.B. (1998). Recombinant adeno-associated virus vector: Use for transgene expression and anterograde tract tracing in the CNS. Brain Res. **793,** 169–175. [In Process citation]

CLARK, K.R., SFERRA, T.J., and JOHNSON, P.R. (1997). Recombinant adeno-associated viral vectors mediate long-term transgene expression in muscle. Hum. Gene Ther. **8,** 659–669.

DUAN, D., FISHER, K.J., BURDA, J.F., and ENGELHARDT, J.F. (1997). Structural and functional heterogeneity of integrated recombinant AAV genomes. Virus Res. **48,** 41–56.

DUAN, D., SHARMA, P., YANG, J., YUE, Y., DUDUS, L., ZHANG, Y., FISHER, K.J., and ENGELHARDT, J.F. (1998a). Circular intermediates of recombinant adeno-associated virus have defined structural characteristics responsible for long term episomal persistence in muscle. J. Virol. **72,** 8568–8577.

DUAN, D., YUE, Y., YAN, Z., MCCRAY, P.B., and ENGELHARDT, J.F. (1998b). Polarity influences the efficiency of recombinant adeno-associated virus infection in differentiated airway epithelia. Hum. Gene Ther. **9,** 2761–2776.

DUAN, D., YAN, Z., YUE, Y., and ENGELHARDT, J.F. (1999). Structural analysis of AAV circular intermediates (submitted).

FERRARI, F.K., SAMULSKI, T., SHENK, T., and SAMULSKI, R.J. (1996). Second-strand synthesis is a rate-limiting step for efficient transduction by recombinant adeno-associated virus vectors. J. Virol. **70,** 3227–3234.

FISHER, K.J., GAO, G.P., WEITZMAN, M.D., DEMATTEO, R., BURDA, J.F., and WILSON, J.M. (1996). Transduction with recombinant adeno-associated virus for gene therapy is limited by leading-strand synthesis. J. Virol. **70,** 520–532.

FLOTTE, T.R., AFIONE, S.A., and ZEITLIN, P.L. (1994). Adeno-associated virus vector gene expression occurs in nondividing cells in the absence of vector DNA integration. Am. J. Respir. Cell Mol. Biol. **11,** 517–521.

HIRT, B. (1967). Selective extraction of polyoma DNA from infected mouse cell cultures. J. Mol. Biol. **26,** 365–369.

KAPLITT, M.G., LEONE, P., SAMULSKI, R.J., XIAO, X., PFAFF, D.W., O'MALLEY, K.L., and DURING, M.J. (1994). Long-term gene expression and phenotypic correction using adeno-associated virus vectors in the mammalian brain. Nature Genet. **8,** 148–154.

KEARNS, W.G., AFIONE, S.A., FULMER, S.B., PANG, M.C., ERIKSON, D., EGAN, M., LANDRUM, M.J., FLOTTE, T.R., and CUTTING, G.R. (1996). Recombinant adeno-associated virus (AAV-CFTR) vectors do not integrate in a site-specific fashion in an immortalized epithelial cell line. Gene Ther. **3,** 748–755.

KOEBERL, D.D., ALEXANDER, I.E., HALBERT, C.L., RUSSELL, D.W., and MILLER, A.D. (1997). Persistent expression of human clotting factor IX from mouse liver after intravenous injection of adeno-associated virus vectors. Proc. Natl. Acad. Sci. U.S.A. **94,** 1426–1431.

KOTIN, R.M., MENNINGER, J.C., WARD, D.C., and BERNS, K.I. (1991). Mapping and direct visualization of a region-specific viral DNA integration site on chromosome 19q13-qter. Genomics. **10,** 831–834.

KOTIN, R.M., LINDEN, R.M., and BERNS, K.I. (1992). Characterization of a preferred site on human chromosome 19q for integration of adeno-associated virus DNA by non-homologous recombination. EMBO J. **11,** 5071–5078.

LEWIS, P.F., and EMERMAN, M. (1994). Passage through mitosis is required for oncoretroviruses but not for the human immunodeficiency virus. J. Virol. **68,** 510–516.

LYNCH, C.M., HARA, P.S., LEONARD, J.C., WILLIAMS, J.K., DEAN, R.H., and GEARY, R.L. (1997). Adeno-associated virus vectors for vascular gene delivery. Circ. Res. **80,** 497–505.

McCOWN, T.J., XIAO, X., LI, J., BREESE, G.R., and SAMULSKI, R.J. (1996). Differential and persistent expression patterns of CNS gene transfer by an adeno-associated virus (AAV) vector. Brain Res. **713,** 99–107.

MIAO, C.H., SNYDER, R.O., SCHOWALTER, D.B., PATIJN, G.A., DONAHUE, B., WINTHER, B., and KAY, M.A. (1998). The kinetics of rAAV integration in the liver. Nature Genet. **19,** 13–15. [Letter]

MILLER, D.G., ADAM, M.A., and MILLER, A.D. (1990). Gene transfer by retrovirus vectors occurs only in cells that are actively replicating at the time of infection. Mol. Cell. Biol. **10,** 4239–4242.

PONNAZHAGAN, S., ERIKSON, D., KEARNS, W.G., ZHOU, S.Z., NAHREINI, P., WANG, X.S., and SRIVASTAVA, A. (1997). Lack of site-specific integration of the recombinant adeno-associated virus 2 genomes in human cells. Hum. Gene Ther. **8,** 275–284.

RICHARDSON, W.D., and WESTPHAL, H. (1981). A cascade of adenovirus early functions is required for expression of adeno-associated virus. Cell **27,** 133–141.

RUSSELL, D.W., ALEXANDER, I.E., and MILLER, A.D. (1995). DNA synthesis and topoisomerase inhibitors increase transduction by adeno-associated virus vectors. Proc. Natl. Acad. Sci. U.S.A. **92,** 5719–5723.

SAMULSKI, R.J., CHANG, L.S., and SHENK, T. (1987). A recombinant plasmid from which an infectious adeno-associated virus genome can be excised in vitro and its use to study viral replication. J. Virol. **61,** 3096–3101.

SAMULSKI, R.J., ZHU, X., XIAO, X., BROOK, J.D., HOUSMAN, D.E., EPSTEIN, N., and HUNTER, L.A. (1991). Targeted integration of adeno-associated virus (AAV) into human chromosome 19. EMBO J. **10,** 3941–3950. [Published erratum appears in EMBO J. 1992;11(3):1228]

STRAUS, S.E., SEBRING, E.D., and ROSE, J.A. (1976). Concatemers of alternating plus and minus strands are intermediates in adenovirus-associated virus DNA synthesis. Proc. Natl. Acad. Sci. U.S.A. **73,** 742–746.

SUMMERFORD, C., and SAMULSKI, R.J. (1998). Membrane-associated heparan sulfate proteoglycan is a receptor for adeno-associated virus type 2 virions. J. Virol. **72,** 1438–1445.

WARD, P., DEAN, F.B., O'DONNELL, M.E., and BERNS, K.I. (1998). Role of the adenovirus DNA-binding protein in in vitro adeno-associated virus DNA replication. J. Virol. **72,** 420–427.

WU, P., PHILLIPS, M.I., BUI, J., and TERWILLIGER, E.F. (1998). Adeno-associated virus vector-mediated transgene integration into neurons and other nondividing cell targets. J. Virol. **72,** 5919–5926. [In process citation]

XIAO, X., LI, J., and SAMULSKI, R.J. (1996). Efficient long-term gene transfer into muscle tissue of immunocompetent mice by adeno-associated virus vector. J. Virol. **70,** 8098–8108.

XIAO, X., XIAO, W., LI, J., and SAMULSKI, R.J. (1997). A novel 165-base-pair terminal repeat sequence is the sole cis requirement for the adeno-associated virus life cycle. J. Virol. **71,** 941–948.

YAKINOGLU, A.O., HEILBRONN, R., BURKLE, A., SCHLEHOFER, J.R., and ZUR HAUSEN, H. (1988). DNA amplification of adeno-associated virus as a response to cellular genotoxic stress. Cancer Res. **48,** 3123–3129.

YAKOBSON, B., KOCH, T., and WINOCOUR, E. (1987). Replication of adeno-associated virus in synchronized cells without the addition of a helper virus. J. Virol. **61,** 972–981.

YANG, C.C., XIAO, X., ZHU, X., ANSARDI, D.C., EPSTEIN, N.D., FREY, M.R., MATERA, A.G., and SAMULSKI, R.J. (1997). Cellular recombination pathways and viral terminal repeat hairpin structures are sufficient for adeno-associated virus integration in vivo and in vitro. J. Virol. **71,** 9231–9247.

Address reprint requests to:
Dr. John F. Engelhardt
Department of Anatomy and Cell Biology
University of Iowa
School of Medicine
51 Newton Road, Room 1-111 BSB
Iowa City, Iowa 52242

E-mail: john-engelhardt@uiowa.edu

Received for publication October 6, 1998; accepted after revision December 16, 1998.